J Membrane Biol (2013) 246:557–570
DOI 10.1007/s00232-013-9568-1

Extracting Curvature Preferences of Lipids Assembled in Flat Bilayers Shows Possible Kinetic Windows for Genesis of Bilayer Asymmetry and Domain Formation in Biological Membranes

Suneyna Bansal · Aditya Mittal

Received: 19 January 2013 / Accepted: 31 May 2013 / Published online: 22 June 2013

Abstract Studies on the assembly of pure lipid components allow mechanistic insights toward understanding the structural and functional aspects of biological membranes. Molecular dynamic (MD) simulations on membrane systems provide molecular details on membrane dynamics that are difficult to obtain experimentally. A large number of MD studies have remained somewhat disconnected from a key concept of amphipathic assembly resulting in membrane structures—shape parameters of lipid molecules in those structures in aqueous environments. This is because most of the MD studies have been done on flat lipid membranes. With the above in view, we analyzed MD simulations of 26 pure lipid patches as a function of (1) lipid type(s) and (2) time of MD simulations along with 35–40 ns trajectories of five pure lipids. We report, for the first time, extraction of curvature preferences of lipids from MD simulations done on flat bilayers. Our results may lead to mechanistic insights into the possible origins of bilayer asymmetries and domain formation in biological membranes.

Keywords Membrane dynamics · Membrane domain · Molecular dynamic simulation · Bilayer · Shape parameter · Membrane curvature

Electronic supplementary material The online version of this article (doi:10.1007/s00232-013-9568-1) contains supplementary material, which is available to authorized users.

S. Bansal · A. Mittal (✉)
Kusuma School of Biological Sciences, Indian Institute of Technology Delhi, New Delhi, India
e-mail: amittal@bioschool.iitd.ac.in

Introduction

Understanding the origins of the first compartmentalized systems that sustained units of life (cells), with subsequent development of intracellular organelles, is central to biology (Cavalier-Smith 2000; Martin and Muller 1998; Rasmussen et al. 2009). Currently, it is well appreciated that several structural and functional aspects of biological compartments are dictated by membrane curvatures that result from interactions between membrane proteins, lipids and other forces experienced by/applied to the membrane components (Chernomordik and Kozlov 2003; Zimmerberg and Kozlov 2006). At the same time, an increasing amount of literature is evolving to decouple (1) the individual contributions of lipid and nonlipid components and (2) the biochemical and biophysical contributions of each of the membrane constituents, in order to better understand how the structural aspects of membranes lead to functional properties, a concept well established for proteins. For example, the role of specific lipids in intracellular trafficking (Mukherjee et al. 1999; Roux et al. 2005); observation of organelle-specific lipid compositions (Asp et al. 2009; Meer and de Kroon 2011; Pecheur et al. 2002); possible roles of lipids in governing intracellular dynamics, domain formation, vesicular sizes, budding, fusion and fission (Chernomordik et al. 1985, 1995; Mittal et al. 2002; Christian et al. 2009; Collins and Keller 2008; Mittal and Grover 2010) and more recently even viral membrane fusion (Zaitseva et al. 2010) have emphasized the importance of nonprotein and primarily lipid-based aspects of biological membranes.

Experimental efforts to understand the formation of biological compartments led to the development of liposomes (Bangham 1972). These efforts were complemented by the elegant conceptual development of the hydrophobic

effect based on experimental data aimed at understanding amphipathic self-assembly in an aqueous environment (Tanford 1973, 1978). Around the same time, the theory of elasticity in membranes was formulated by Helfrich (1973), a contribution that continues to play a key role in understanding the parameters that govern the membrane curvatures responsible for providing a variety of structural and functional properties to biological compartments. To gain insight into the molecular origins of the hydrophobic effect, the elastic theory of membranes and assembly of a variety of compartmental structures, the concept of "shape parameter" was introduced by Israelachvili et al. (1976). Subsequently, several elegant studies have investigated the possible role of the molecular shapes of lipid constituents on whole-cell morphology (Christiansson et al. 1985) or how individual lipid constituents prefer to localize into specifically curved membranes, thereby stabilizing membrane structures with a given curvature, and/or to form different phases/domains within what was assumed to be a single membrane (Lee et al. 1991; Lipowsky 1992; Marsh 1996).

While the above developments continue to guide our current efforts in understanding structure–function relationships for lipids in biological membranes, they provide negligible insights into membrane dynamics. To overcome this limitation, the first molecular dynamic (MD) simulation on lipids was reported by Kox et al. (1980). Subsequently, several MD simulations have been performed on different lipid systems and for different simulation times, to understand the dynamics of membranes formed by pure lipid systems (Dickey and Faller 2008a, 2008b; Feller et al. 1997; Gurtovenko et al. 2004; Klauda et al. 2010; Marrink et al. 1998; Patra et al. 2003, 2004; Tieleman and Berendsen 1998; Tieleman et al. 1999; Suits et al. 2005; Zhao et al. 2007). Although there are a few reports on atomistic MD simulations of micelles (Lazaridis et al. 2005; Tieleman et al. 2000), a majority of the studies were carried out on flat lipid membranes, of about 128–512 lipids ($\sim$6–8 nm in linear size), which corresponds to a small flat patch on giant unilamellar vesicles (GUVs). This is because of the computational limitations toward handling very large system sizes and long timescales for exploring lipid shape preferences to generate various preferred curvatures using atomistic MD simulations. For example, only recently some computational studies have explored the possible coupling between the shapes of individual lipid constituents and the overall curvature of the membranes (Apajalahti et al. 2010; Cooke and Deserno 2006; Davis et al. 2007). However, the large body of literature with MD simulation data on pure lipid systems has not been able to correlate the observed dynamics in flat bilayers to the concepts of shape parameter of the individual lipids and overall membrane curvature preferred/formed by these lipids. In simpler terms, MD simulation data on "small" and "flat" patches of membranes have remained somewhat disconnected from concepts of the shapes of individual components forming preferential membrane curvatures. The strength of MD simulation data lies in providing mechanistic insights, at a molecular level, that are difficult to obtain either experimentally or using nondynamic theoretical concepts applicable to average system properties. Therefore, in this work, we asked whether these atomistic MD simulation data on flat bilayers could provide crucial information on the dynamics of the shapes of individual lipid components leading to specific curvature preferences, in spite of the symmetry, flatness and small size of the membrane patches. By carrying out an unprecedented large-scale, rigorous analysis of MD simulation data from 26 flat pure lipid membranes with different lipids and for different simulation times and five complete lipid trajectories of 20 ns each (100 frames), we report the remarkable extraction of curvature preferences of individual lipids in spite of the "flatness" of the systems analyzed. Our work unifies atomistic MD simulation results on flat membranes with the concepts of the role of lipids in curved biological membranes for the first time, to the best of our knowledge. We also provide a possible mechanism on how flat patches of membranes may develop segregated domains/phases, and possibly nanoscale curvatures, due to a localization of initially distributed/mixed single-lipid molecules with specific shape parameters.

Methods

Lipid Structure Preparation

Twenty-six minimized membrane patches of eight different membrane phospholipids and bilayer trajectories of five different phospholipids were retrieved from various resources (see Supplementary Table S1). Klauda et al. (2010) reported simulations of five different bilayers for 35–40 ns including equilibration runs of 15–20 ns, and these results were found to be correlated with the experimental parameters, which include surface area per lipid, order parameter, form factor and electron density of bilayers. Hence, we also included these postequilibration trajectories of five different membrane patches in our study. A preequilibrated membrane patch (or input membrane at 0 ns) was generated under comparable conditions (Klauda et al. 2010) for each trajectory using the membrane builder module of the CHARMM-GUI Web-based interface (Jo et al. 2009). Coordinates of each molecule were processed to add hydrogen atoms and solvent molecules were removed using PyMOL (Schrödinger, Bangalore, India) (Fig. 1a–c). Coordinate information of each

lipid was then extracted from the complete membrane pdb file. Using coordinate information on each lipid, first line diagrams were created using a color code to distinguish various connections among atoms with MATLAB (MathWorks, Natick, MA) (Fig. 1d). Then, using van der Waals radius information (Allen 2002) and treating the x, y and z positions of each atom as their centers, a sphere was drawn around each of them to get their three-dimensional (3D) van der Waals spherical structures (Fig. 1e). To get a more refined volumetric representation with fewer coordinates, van der Waals surfaces were drawn by eliminating common regions among spheres for each lipid (Fig. 1f). These van der Waals surfaces showed the actual volume occupied by each lipid and were used as the final structures to calculate their shape parameter.

Shape Parameter Calculation

Selection of the optimized symmetry axis and determination of the slant line were two prerequisites for the complete enclosure of these lipid structures into a molecular shape. A geometrical axis was drawn by joining the centroids of the head and tail regions of each molecule (see Fig. 1g, h). For this, a median function was used, separately, for the x, y and z coordinates of the head and tail regions of each lipid in MATLAB. The resulting head and tail centroid points were then joined to get the central geometrical axis. For the ease of further calculations and slant line optimization, we rotated our axis along the lipid molecule to make its configuration normal to the x- and y-axes or parallel to the z-axis (considering the fact that the head should remain in the positive z-direction compared to the tail or the lipid should be in an upside-down position and not the reverse). To get the final configuration, stepwise rotation was performed, once around the y-axis and then around the x-axis (for details, see supplementary material, Fig. S1). The rotated geometric axis was then easily extended toward the topmost head point and the bottommost tail point, to span the entire length of the molecule.

Now, for selecting the optimized slant line and for the complete enclosure of each lipid, we first searched for the farthest atomic coordinate point of the lipid from its central axis and called it the "reference point". Then, a line perpendicular to the main axis to this reference point was drawn and termed its "reference radius" (for details, see supplementary material, Fig. S2). Several slant lines were drawn by joining this reference point separately with each surface point of the lipid molecule. Using MATLAB, the line with the maximum slant angle with respect to the reference radius was selected to be the appropriate slant line as a 360° rotation of this line around the main axis can completely enclose the whole structure with minimum occupied volume. This slant line was then extended to span the entire length of the lipid molecule. Taking this slant line, we wrapped the lipid structure to get the appropriate geometries. If the head radius was found to be greater than the tail radius, an "upright truncated cone" was formed (Fig. 1i). If the head radius was less than the tail radius, the result was an "inverted truncated cone" (Fig. 1j). We always found some difference in the values of the head and tail radius, or we can say that we never found a cylindrical shape for any lipid structure. These molecular shapes were then used to calculate the "packing parameter" or "shape parameter" for each lipid. For this, we used two well-defined definitions of this parameter from the literature, by Israelachvili et al. (1976) and Marsh (1996), respectively, as

$$S = \frac{v}{al} \tag{1}$$

where v is the hydrophobic volume of the lipid, a is the head–tail interfacial area and l is the extended length of the hydrophobic tails of the lipids, and

$$S = \frac{V}{aL} \tag{2}$$

where V is the volume of the complete lipid molecule, a is the head–tail interfacial area and L is the complete length of the lipids.

Results and Discussion

Computational Control: "Average" Shape Parameter Value in Flat Bilayers is 1

We first collected structural (atomistic) details of each individual lipid molecule from every simulated membrane patch listed in Supplementary Table S1. Then, we developed an algorithm to characterize the shapes of various lipid constituents of biological membranes. We found predominantly two different shapes for each phospholipid, one with a larger head group area than its acyl tails that formed upright truncated cones and the other with a smaller head group area than its acyl tails that formed inverted truncated cones. For each of the lipids, we parameterized these shapes in terms of its shape parameter, S, using both Eqs. 1 and 2 (see "Methods" section). The first step was to test the correctness of our parameterization, i.e., calculation of shape parameters. To do so, we calculated the average shape parameter for phospholipids in each of the patches analyzed. Since the data analyzed were from simulations on flat bilayers only, we expected the average shape parameter of all the phospholipids to be $S = 1$. For example, if the total lipids in a simulation were 64, with 32

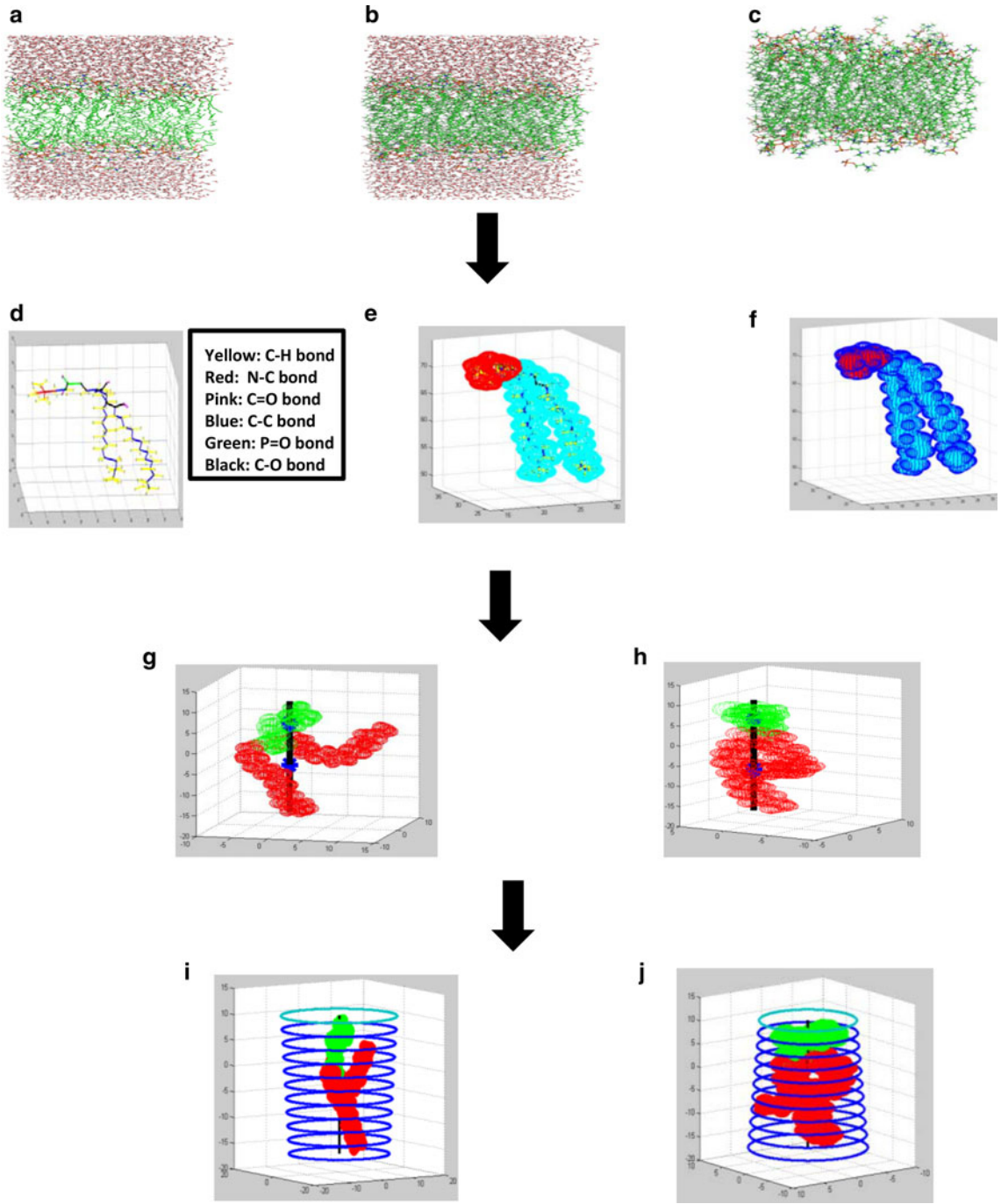

Fig. 1 Overview of the methodology. **a** Simulated lipid bilayer, **b** bilayer after addition of hydrogen atoms, **c** bilayer after removal of solvent molecules, **d** structure of extracted lipid drawn in MATLAB, **e** van der Waals spherical representation and **f** van der Waals surface representation. Only *dark blue* region depicts the surface of the lipid; *cyan-colored* tail region and *red* head region show deleted common regions among spheres. **g**, **h** Axis drawn by joining of the centroid of the head region to the centroid of the tail region of the molecule. **i** *Upright*, truncated, cone-shaped lipid; **j** *inverted*, truncated, cone-shaped lipid (Color figure online)

each in the upper and lower monolayers, we expected the average shape parameter of all these lipids to be 1, regardless of the type of lipid or the time of simulation, since the bilayers are seen to be flat throughout the MD simulations. Note that as these bilayers are symmetric in nature, we called them "upper" and "lower" monolayers with respect to their lipid configuration in each layer, which means that if it contained all of the lipids whose head regions were in the positive z-direction compared to the tail points, we took this monolayer as the upper leaflet

and vice versa, to see whether this symmetry would induce similar results in terms of the shape parameter distribution of lipids in each monolayer. As expected, we found the average shape parameter to be ~1.0 regardless of the method of calculation of the shape parameter, the type of lipid and the presence of the lipid in the upper or lower leaflet (Fig. 2). This consistency in the average shape parameter was also observed for membrane patches simulated for different time periods and maintained from 0 ns (preequilibrated patches) to the complete course of trajectories for all five phospholipids (Supplementary Figs. S3, S4). These results provided an internal control to our calculations in terms of predicted and calculated values of *S* in flat membranes.

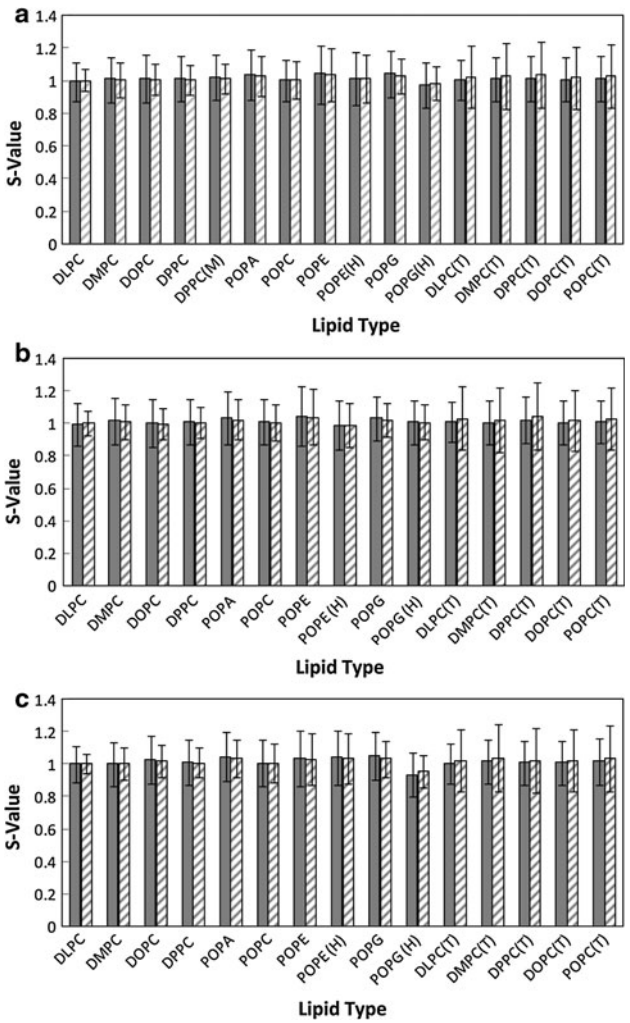

Fig. 2 Average shape parameter (*S*) as a function of phospholipids. **a** Average *S* values of whole membrane patch calculated from Eq. 1 (*solid bars*) and Eq. 2 (*striped bars*), for *n* (total number of lipids), see Table 1. **b** Average *S* values for upper monolayer. **c** Average *S* values for lower monolayer. *Error bars* represents standard deviation. *M* monolayer, *H* heterogeneous patch of POPE and POPG, *T* average *S* value from the 20-ns-long trajectory (excluding preequilibration run) of each lipid molecule

Extraction of Curvature Preferences of Lipids in Flat Bilayers

Experimental observations of nanoscale (Sharma et al. 2004), submicron-scale (Kusumi et al. 2004) and micron-scale (Veatch and Keller 2003) clusters of lipids, varying from ~4–6 nm to ~1 μm in size and consisting of fewer than five molecules to several hundreds of lipid molecules, have been reported. Clusters of lipids in these membranes have been observed either as small shells around specific proteins or as segregated lipid patches with or without other nonlipid constituents, often referred to as "rafts" or "domains." In terms of dynamics, observations of these varying clusters of lipids have been on much longer timescales than the timescales employed for MD simulations. Further, it is well appreciated from the existing literature that *S* is not a dynamic parameter with any lipid-specific kinetics. Thus, although periodic boundary conditions do not allow large curvature changes (Kupiainen et al. 2005) and the presence of symmetrical monolayers prevents the formation of large lipid clusters through some of the proposed mechanisms such as the development of a difference in line tensions between lipids (Baumgart et al. 2003), we were interested in finding whether the lipids adopt their preferred conformation (expressed in terms of *S*) soon after assembly or membrane formation, independent of their time of simulation during MD. Therefore, we formulated a straightforward hypothesis to unify the experimental observations with MD simulation data and the concept of *S*: for a given lipid, there must be a consistent signature value (either *S* or some derivative of *S*) for at least some molecules within the flat membranes of MD simulations. Thus, while MD simulations show flat membranes with average $S \sim 1.0$ for all lipids during the whole simulations, there must be at least some single lipid molecules with substantial deviations from $S = 1.0$. These molecules should be homogenously distributed in the flat membranes. Further, their deviations from $S = 1.0$ must be compensated by some other molecules within the flat membranes since the MD simulations do not show development of any overall curvature.

To investigate the above, we calculated the ratio of upright truncated cones versus inverted truncated cones for each of the membrane lipids in each of the membrane patches. Figure 3 shows that this ratio ranges from 0.7 to 1.5 for all the membranes, regardless of the method of calculation of *S*. Note that the straight line in the graphs represents a ratio of 1.0, a theoretical case in which the membrane remains flat by having the exact compensation of upright and inverted truncated cones (only possible for flat membranes when each upright and inverted truncated cone is placed alternatively, resulting in continuous flatness). These results were clearly indicative of the presence

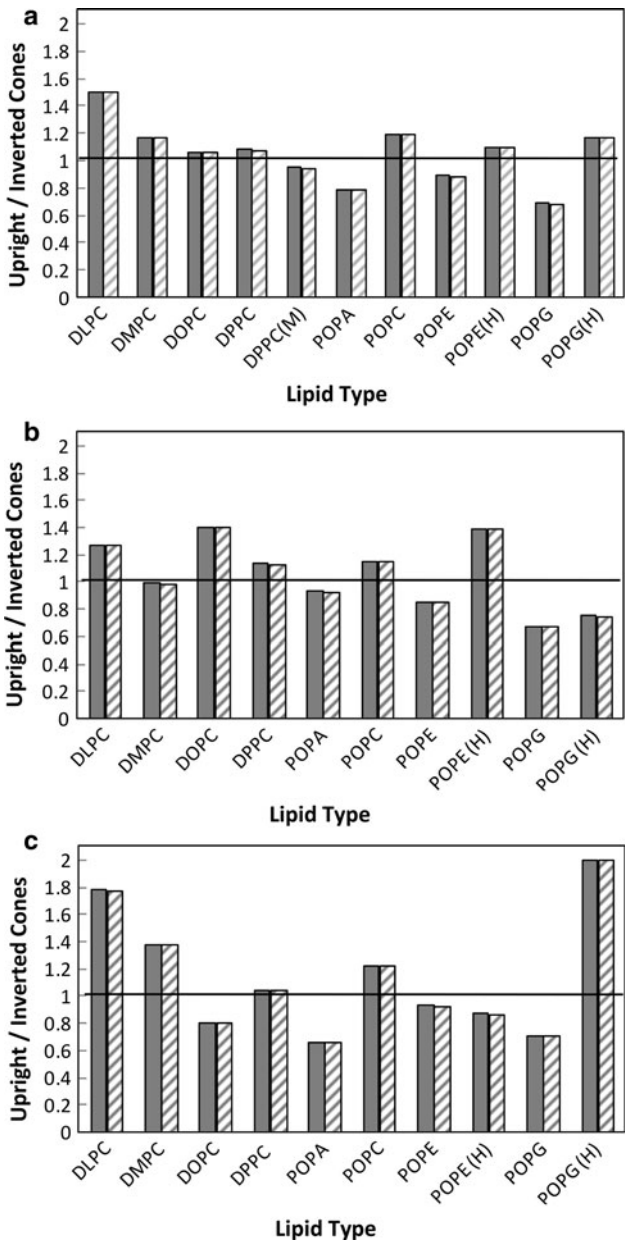

Fig. 3 Ratio of upright and inverted truncated cones of membrane phospholipids. For each of the lipids, total numbers of upright and inverted truncated cones, defined by *S* value, were counted from all of its patches and then ratios were plotted as a function of lipid. *Solid straight line* represents equal numbers of upright and inverted truncated cones. *S* values calculated by Eqs. 1 (*solid bars*) and 2 (*striped bars*) resulted in identical ratios. **a** Ratio for membrane patch, **b** ratio for upper monolayer and **c** ratio for lower leaflet. *M* monolayer, *H* heterogeneous patch of POPE and POPG

of curvature preference for several lipids. In most of the cases, this ratio correlated well with the predicted/expected effective molecular shape of these lipids, as shown in Table 1 (*S* 4, 9 and 10, or DOPC, POPE[H] and POPG[H], respectively, are the exceptions, see next section). Interestingly, deviation from the ratio of 1.0 was observed to be slightly differently distributed in the upper (0.67–1.4) and lower (0.66–2.0) monolayers. This result provides a possible insight into the kinetic/dynamic dependence of the development of membrane asymmetry in monolayers (see next section).

Here, it is important to note that simulated membranes may undergo (possibly substantial) area and volume fluctuations during MD studies. Thus, analysis of individual lipid shape parameters in a single snapshot may not capture signature ratio values accurately or representatively. To overcome this limitation of our work described thus far, we also analyzed the signature ratio values for the complete trajectories of five different phospholipids generated under comparable conditions (see material, Table S1). The key results were (1) control calculations, i.e., an average ratio of ~ 1 for each lipid in the preequilibrated membrane, were in agreement with our previous findings, and (2) the values of the ratio were found to fluctuate from 0.6 to 2.1 for bilayers and from 0.4 to 3.5 for both the upper and lower monolayers, during the whole course of simulation (see Fig. 4a–c). Now, to check whether the signature of ratio values was emerging from the simulations, we calculated the fraction of time in which the shape ratio was greater than or equal to 1 or less than 1 (Fig. 4d). Note that here the straight line at a ratio of 1 for a particular lipid depicts that its signature value for *S* is not captured. To our satisfaction, we found that ratio results from these trajectories correlated well with our earlier results as well as the existing literature (see Fig. 4d; Table 1). Interestingly, higher fluctuations observed in the values of the ratio in the upper and lower monolayers (Fig. 4a–c) may indicate possible kinetic windows for the origin of membrane asymmetry.

Dynamics of the Shape Parameter and Its Thermodynamic Significance

While considering amphipathic self-assembly in aqueous systems, it is well appreciated that critical micellar concentration and critical compartmentalization concentration are thermodynamic parameters (Mittal and Grover 2010; Tanford 1973, 1978). This implies that the formation of molecular micelles or compartments occurs only at (and beyond) the critical concentration of amphipathic molecules (i.e., number of amphipathic molecules in a closed aqueous system). However, it is quite underappreciated that *S* also must be closely coupled with these thermodynamic concepts based on the hydrophobic effect. To illustrate this, it is important to point out that while studies involving MD simulations on lipid systems rigorously analyze some important contributors of curvature in large-scale structures like the length of acyl chains, their tilt and splay and areas of head group per lipid, they do not address

Table 1 Comparative analysis of expected molecular shapes of membrane lipids

S	Lipid	Expected shape from literature	Expected shape from this work Bilayer (upper/lower monolayer)	Expected shape from full trajectories Bilayer (upper/lower monolayer)
1	DLPC	U[a]	U (U/U)	U (U[e]/U)
2	DMPC	U[a]	U ($\sim$1/U)	U (U/U[e])
3	DPPC	U[a]	U[e] (U/$\sim$1)	U (1/U)
4	DOPC	I[b,e]	U[e] (U/I)	U (U/U[e])
5	POPC	U[c,e]	U (U/U)	U[e] (U/U)
6	POPA	I[c]	I (I[e]/I)	–
7	POPE	I[c]	I (I/1[e])	–
8	POPG	I[d]	I (I/I)	–
9	POPE(H)	I[c]	U (U/I)	–
10	POPG(H)	I[d]	U (I/U)	–
11	DPPC(M)	NA	I[e]	–

Predicted molecular shapes of the membrane lipids from the literature compared with our predicted shapes

NA not available, *U* upright and *I* inverted truncated conical shapes

[a] Kumar (1991)

[b] Chernomordik and Kozlov (2003)

[c] Osman et al. (2011)

[d] Jimenez-Monreal et al. (1998)

[e] Slightly upright or slightly inverted (in terms of *S* value). $\sim$1 means ratio value near 1

S per lipid or an average. In fact, conceptually *S* is defined only after self-assembly has taken place; i.e., it is a parameter applicable to the lipid shape in a preexisting assembled system. Thus, *S* essentially provides the possible configuration of a self-assembled system that will be formed beyond a certain concentration by an amphipathic molecule. However, what would be the dynamics of *S* for a single lipid or a number of lipids below the critical self-assembly concentrations in aqueous solutions? Can *S* have any predictive importance rather than just post facto analytical significance? Essentially, analogous to the hydrodynamic radius of other polymeric systems such as proteins, can *S* provide some intrinsic information about an amphipathic molecule? Can *S* emerge soon after the assembly formation, or is there any minimal time for *S* to appear during MD simulations?

The above questions were partly answered by closely inspecting Table 1. The ratios of upright versus inverted shapes for DOPC, POPE(H) and POPG(H) observed from MD simulation data of flat bilayers do not agree with their known shape preferences. A detailed analysis of MD simulation data for each lipid, with different times of MD simulations, provided a remarkable insight into this disagreement as well as answers to the above questions. Figure 5 shows the observed curvature preferences, in terms of ratio of upright versus inverted truncated cones, for different lipids as a function of MD simulation time. Clearly, while for some lipids curvature preferences are observed regardless of simulation time (e.g., POPC and POPA in Fig. 5a), for others lipid curvature preferences vary with the simulation time (e.g., DPPC in Fig. 5a). Further, the curvature preferences based on individual monolayers show a dynamic behavior (Fig. 5b, c). These observations are highlighted for lipids on which MD simulation times were different up to 100 ns (see supplementary material, Figs. S5, S6). Figure 4 also reveals that the minimum time window required to extract *S* reliably from a DLPC bilayer (2 $\times$ 36 molecules) was about 21 ns, while for DMPC and DPPC longer time frames of 31 ns or more are required and for POPC and DOPC an equilibration run of at least more than 35 ns was required to get the stable expected ratio value throughout the trajectory. The following inferences are drawn from these observations: (1) the dynamics of *S* are captured in MD simulations, (2) these dynamics indicate possible concentration dependence of *S*—fluctuations are proportional to the size of MD simulation membrane patches (i.e., number of lipids), (3) these dynamics also vary with the unsaturation of lipid molecules—more unsaturation results in the need for either large-sized membranes or longer simulation times for small-sized bilayers and (4) the dynamics of nonsymmetrical curvature preferences in individual monolayers clearly point toward a possible mechanism of origin of membrane asymmetries for even homogenous systems in the context of cellular environments. In the presence of other constituents/forces/ligands on either monolayer, curvature fluctuations within nanosecond scales can be stabilized, leading to asymmetry in bilayers.

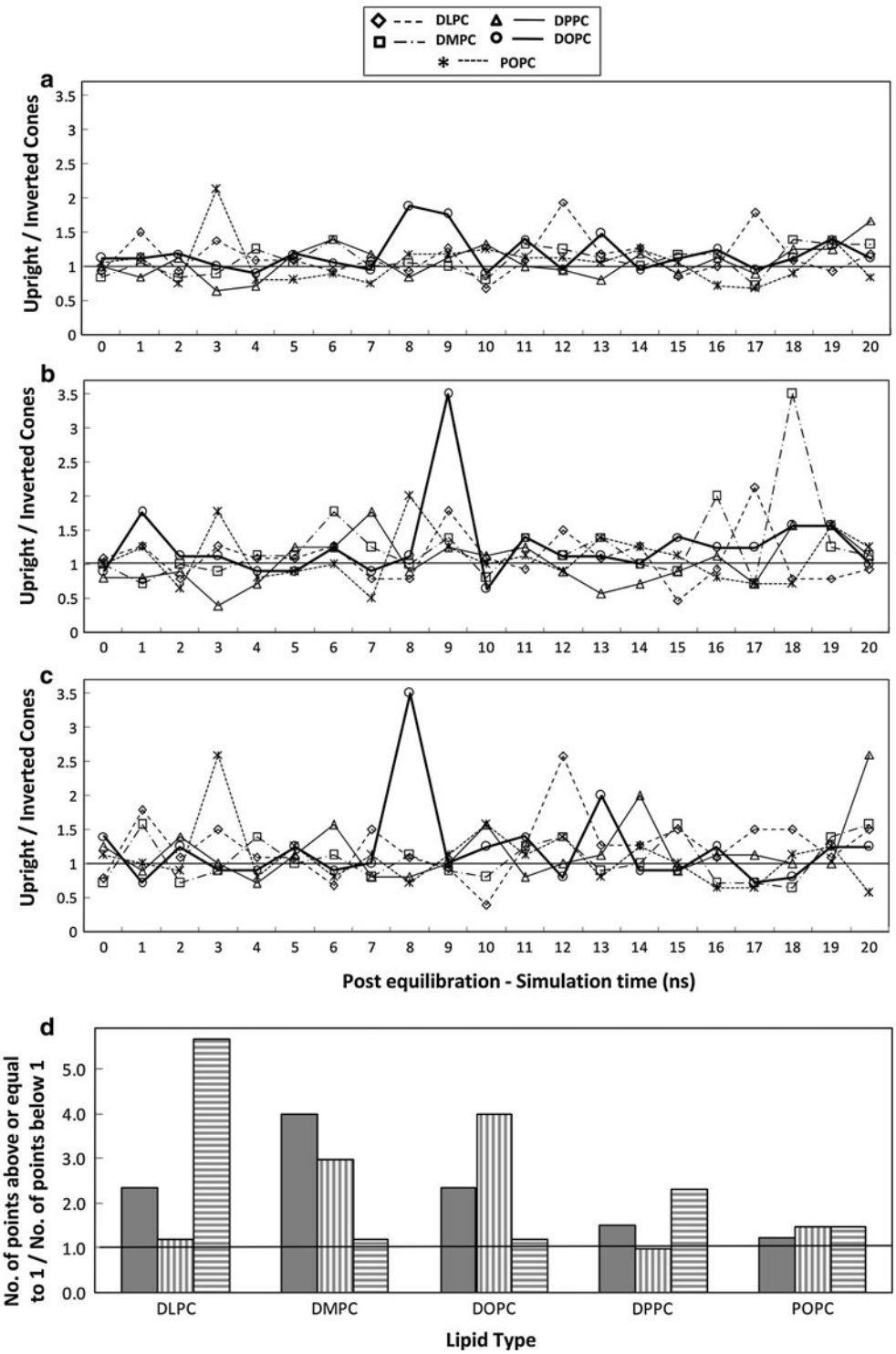

Fig. 4 Ratio variation in whole trajectories of phospholipids with respect to their simulation time. Simulation time represents postequilibration run for each of the membrane patches. For DLPC, DMPC and DPPC, 40-ns-long simulations (excluding initial 20-ns-long preequilibration run) were analyzed; and for DOPC and POPC, 35-ns-long simulations (excluding initial 15-ns-long preequilibration run) were analyzed. For each of the lipids, total numbers of upright and inverted truncated cones were counted from its single patch, and then ratios were plotted against each of them (for details, see material, Table S3). 0 ns represents the ratio for the preequilibrated membrane patch (see "Methods" section). As shown in Fig. 6, Eqs. 1 and 2 resulted in identical values; thus, a single value is shown here. **a** Ratio for whole membrane patch, **b** ratio for upper monolayer and **c** ratio for lower monolayer. In **a–c**, the *solid straight line* at ratio 1 represents the flat curvature. For each lipid, the numbers of snapshots for a ratio value greater than, equal to or less than 1 were determined; then, their ratios were plotted against each lipid type. **d** Ratio of the number of points ≥ 1 to the number of points <1 for whole bilayer (*solid bars*), upper monolayer (*vertical striped bars*) and lower monolayer (*horizontal striped bars*). Here, a ratio of 1 depicts the nonemergence of the signature of the shape parameter during the given trajectory

Here, it is important to emphasize that in spite of the dynamics of *S*, the combination of all of the MD simulation data on flat bilayers (i.e., analysis only as a function of lipid type and ignoring time of MD simulation) does extract specific curvature preferences, thereby providing the shape parameter with a predictive significance (Figs. 3, 4d; Table 1).

Curvature Formation Inferred by Proportional Variation in the Molecular Shapes of Lipids

It has been proposed that (nano)domains of lipids can be formed due to localized mismatches in lipids with respect to their composition, height or "shape" (Johannes and Mayor 2010). Surprisingly, such proposals are disconnected from

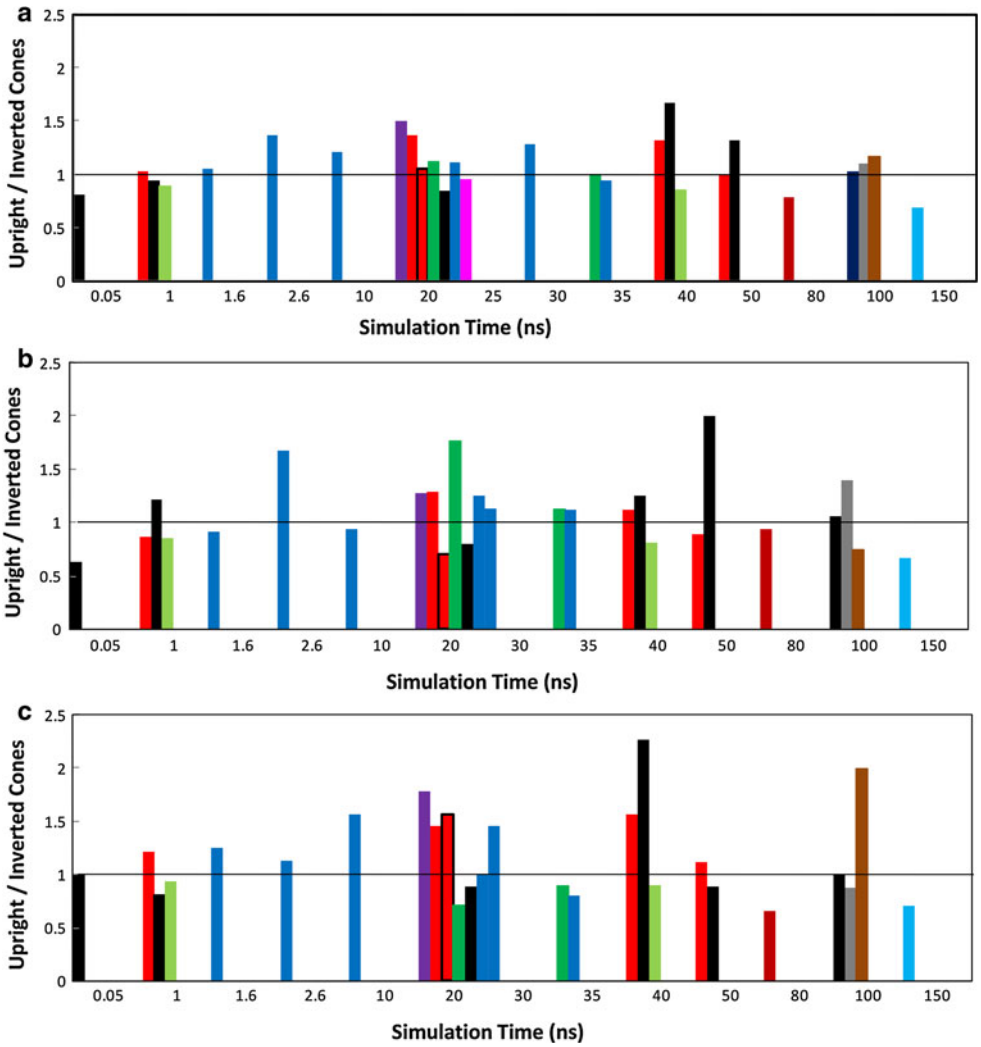

Fig. 5 Ratio of upright and inverted truncated cones of membrane phospholipids as a function of simulation time. For each of the lipids, total numbers of upright and inverted truncated cones were determined from a single patch and then ratios were plotted against each of them (for details, see supplementary material, Table S2). *Solid straight line* at ratio 1 represents the flat curvature. As shown in Fig. 5, Eqs. 1 and 2 resulted in identical values; thus, a single value is shown here. **a** Ratio for whole membrane patch, **b** ratio for upper monolayer and **c** ratio for lower monolayer. Color code: DLPC (*purple*), DMPC (*red*), DOPC (*dark green*), DPPC (*black*), DPPC monolayer patch (*pink*), POPA (*dark red*), POPC (*dark blue*), POPE (*green*), POPE in mixed patch (*gray*), POPG (*blue*) and POPG in mixed patch (*brown*). *Red bar with black outline* represents two different DMPC bilayer patches simulated for the same time period of 20 ns (Color figure online)

the established concept of shape parameter. The concept of "shape" has been explored only visually rather than quantitatively in terms of the well-defined shape parameter. Thus, we asked whether data from atomistic MD simulations can allow a rigorous quantitative investigation of "shape mismatch" as a leading mechanism for initiating and/or stabilizing membrane lipids into (nano)domains, with further assistance from other membrane constituents (e.g., proteins). So, here, we predicted possible curvatures depending upon the ratio difference of upright truncated cones and inverted truncated cones (Fig. 6 and supplementary material, Tables S2, S3). Temporal development of shape variation in each of the five trajectories can be clearly seen in the Supplementary Table S4, which represents the ratio variation of these shapes at intervals of 5 ns. Most of these curvatures are biologically significant structures; for example, b and c represent vesicle or daughter bud formation (Christian et al. 2009) d resembles a hemifusion stalk-like structure or hourglass-shaped curvature (Chernomordik et al. 1985) and e looks like a segregated lipid domain (Cicuta et al. 2007). Other curvatures, like f, g, h and i, seem to represent initial proliferation of budding and invagination on the membrane surface or on endocytic vesicles (Mukherjee et al. 1999). A summary of all possible inferred curvature formations from flat patches of membranes (simulated under different conditions: time, temperature) analyzed here is shown in supplementary material, Fig. S7. The most interesting aspect from this summarization is seen on quantifying the "curvature area" out of whole patch area, by counting the percentage difference in the number of two shapes (upright, inverted) for each leaflet and calculating this as the percent area of curvature. Essentially, the concept is to infer the curvatures if all the upright lipids were together and all the inverted lipids were together in their respective monolayers, how the structures would appear in terms of Fig. 6, rather than appearing flat in the MD simulations with lipids distributed and not clustered.

Remarkably, the following lipid domain formations are directly inferred in this work (supplementary material,

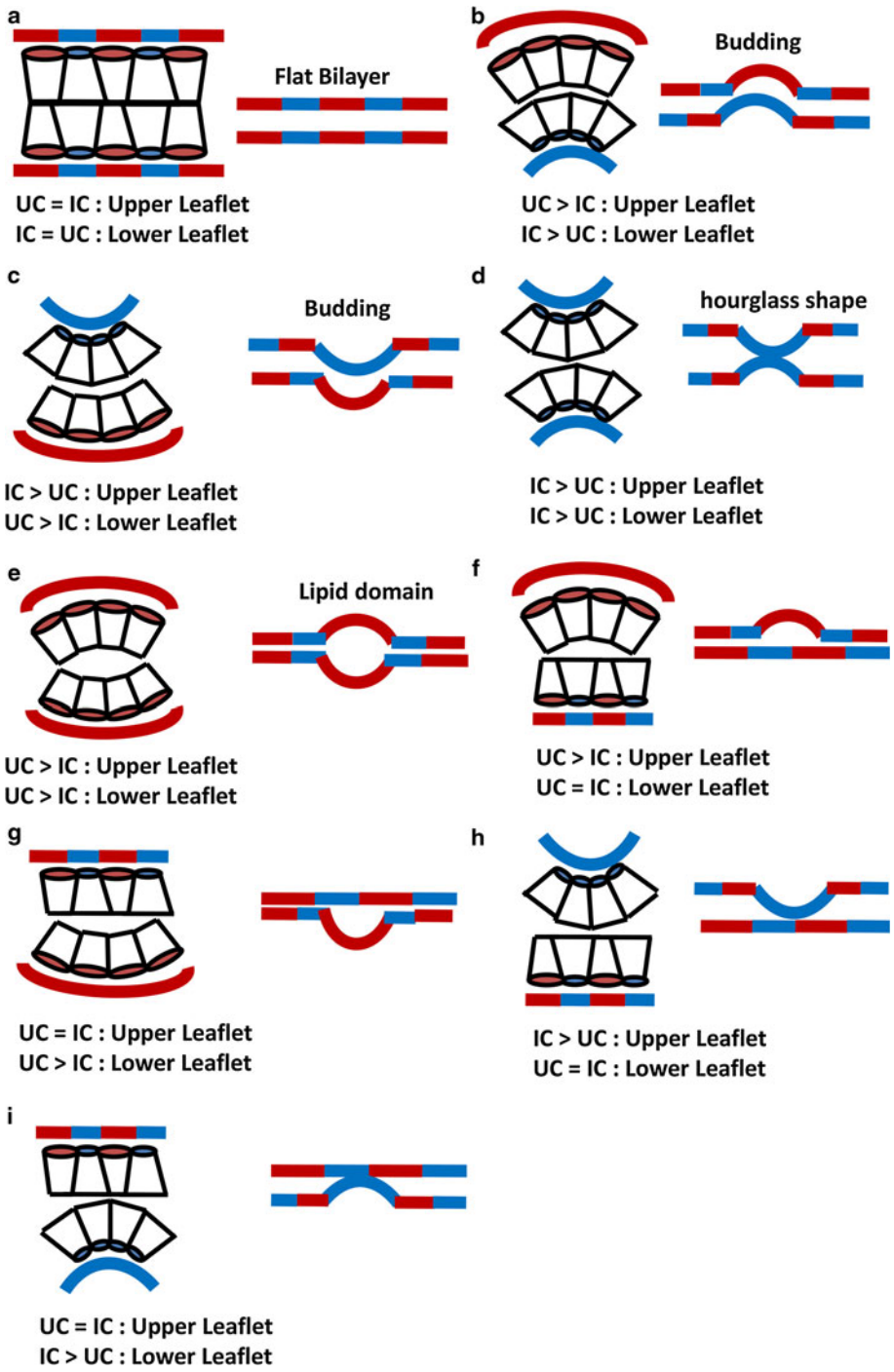

Fig. 6 Possible curvatures depending upon the stoichiometric ratio mismatch in two shapes (*upright and inverted*). Possible curvatures that could result from the aggregation of lipids in a small region(s) of any one and/or both of the monolayers are shown. *UC* upright truncated cones (*red*), *IC* inverted truncated cones (*blue*) (Color figure online)

Fig. S7): (1) positive curvature preferences in both leaflets for dilauroylphosphatidylcholine (DLPC, 12–28 and 2–9 %) from its trajectory, palmitoyl-oleoyl phosphatidylcholine (POPC 9–17 and 0.6–1.7 %) from its trajectory, dipalmitoylphosphatidylcholine (DPPC 4–13 %), dimyristoylphosphatidylcholine (DMPC 1–8 %) from its trajectory and dioleoylphosphatidylcholine (DOPC 4–9 %) from its trajectory; (2) bud-like structure formation for DMPC (7–14 %), DPPC (1–5 %) from its trajectory and DOPC (11–17 %); and (3) hemifusion stalk-like structure for palmitoyl-oleoyl phosphatidic acid (POPA 3–21 %), palmitoyl-oleoyl phosphatidylethanolamine (POPE 3–9 %) and palmitoyl-oleoyl phosphatidylglycerols (POPG 17–20 %). Curvatures formed for a saturated fatty acyl tail containing phosphatidylcholines (PCs) indicate their positive curvature preferences. With decreasing tail length of PCs, we observed a slight increase in the number of upright truncated cones and, hence, increased positive curvature

(Figs. 3, 4d). This is in agreement with the recent observation in which an increase in acyl tail length of PCs accompanied a slight increase in *S* value (Kumar 1991).

Recently, GUVs made of DOPC disordered domain and sphingomyelin- and cholesterol-rich ordered domain were shown to form highly curved, bud-like curvatures from DOPC disordered domain at 25–50 °C using fluorescence microscopy (Baumgart et al. 2003). The timescale for curvature change (or bud formation) was measured to be 0.5 s after the separation of the above two domains. Roux et al. (2005) also reported the preferential segregation of DOPC into disordered domain for the generation of bud and pulling tube formation from vesicles. Our study also predicts the formation of a small bud-like curvature in simulated DOPC bilayer at 30 °C (see supplementary material, Fig. S7a). In trajectory analysis also, most of the time, the DOPC membrane can be predicted to form a bud-like curvature (Fig. S7a). This may imply that although thermodynamic conditions like temperature are favourable for bud formation in the above DOPC patches, introduction of some stabilizing agents (such as other lipid constituents as used in the above experiment) may help in the generation of such small, bud-like structures in flat MD patches simulated for a longer duration of around 1 s. It has been found that phosphatidylethanolamine (PE), phosphatidic acid (PA) and diacylglycerols (DAGs) are important regulators of fusion and fission processes in cellular membranes. PE is known to be involved in the fusion of Golgi membranes (Pecheur et al. 2002). It also helps in disassembly of the contractile ring during cytokinesis (Emoto and Umeda 2000). DAGs are also known regulators of fission of the trans-Golgi network (Asp et al. 2009). PA plays a crucial role in the budding of vesicles and Golgi tubes (Judson and Brown 2009). In our results too, POPE, POPA and POPG showed negative curvature preferences and predicted hourglass-like curvature formation, which mimics the hemifusion stalk formed between two monolayers during the fusion process. DOPG has also been shown to induce negative curvature in various PCs (Szule et al. 2002)—it was observed that unsaturation eases the induction of hexagonal phase formation. With POPC, DOG (DOG:POPC = 1:3) resulted in hexagonal phase formation at 50 °C but a lamellar-hexagonal coexisting phase can be formed at a lower temperature of 22 °C. Also, a phase diagram of POPG in POPC clearly indicates the existence of a cubic phase for this mix, which itself suggested a negative curvature preference for the same (Jimenez-Monreal et al. 1998). The heterogeneous bilayer patch analyzed here contains POPG:POPE = 1:3 and was simulated at 37 °C. We found the possibility of small bud-like curvatures moving upward in a POPE (7–16 %)—rich region and downward bud-like structures in the POPG (14–33 %)—rich region of a heterogeneous patch. This may also imply that the simulation time needs to be long enough to allow lateral mixing of these two lipids to form the final expected curvatures.

Conclusions

MD simulations are extremely useful in developing an atomistic-level understanding of lipid behavior in biological membranes that is difficult to explore through experiments. However, a large body of literature involving some elegant studies on MD simulations of pure lipid membranes has remained disconnected from thermodynamic concepts of the critical compartmentalization concentration of lipid components in forming membranes and the concept of shape parameter. The primary reason for this disconnect has been practical limitations of simulating large system sizes for longer timescales. Hence, atomistic MD simulations usually explore the molecular behavior of lipids in flat membranes, whereas individual membrane lipids have been known to show specific curvature preferences. In this work, we analyzed structural data for individual lipids from MD simulations conducted on 26 flat pure lipid membranes and five complete trajectory profiles of 20 ns each. We analyzed the data in terms of the shapes of individual lipid molecules as a function of (1) type of lipid and (2) time of MD simulation. Regardless of the "flatness" of the systems analyzed, we report, for the first time (to our knowledge), extraction of curvature preferences for individual lipids from simulations done on flat bilayers. While finding results in support of the shape parameter (*S*) being a thermodynamic, rather than a kinetic, parameter, we also report how pure/homogeneous or even heterogeneous lipid bilayers can develop asymmetry between the two monolayers due to time-dependent asymmetrical attributes discovered in the two monolayers from the MD simulation data. Timescales of these asymmetrical attributes are of the order of only a few nanoseconds, thereby indicating that addition of any new component (another molecule or any kind of force) into the system can lead to (1) clustering/domain formation and/or (2) formation of curvatures known to be lipid-specific only in whole lipid systems previously observed for microseconds and higher through coarse-grained models (Schafer and Marrink 2010; Shillcock and Lipowsky 2005) and experiments. To our knowledge, this is the first study indicating such usefulness of atomistic MD simulations on flat bilayers, while for the first time unifying the thermodynamic concept of shape parameter with the kinetic behavior observed in MD simulations.

Finally, it is interesting to consider further applications of the approach developed by us in this work. While this work is focused on understanding curvature preferences of

individual lipids and overall curvatures that may be formed by assembly of these lipids, another important aspect is understanding the phase behavior of membranes, which can be investigated by analyzing the "order parameter." The order parameter is an important contributor to, and provides a measurable signature for, the state or phase of the membranes (Seelig and Seeling 1974). Quantitatively, this parameter is defined as $S_n = (1/2) \times (3\cos^2\theta_n - 1)$, where S_n is the order parameter for nth C–D vector and θ_n is the time-dependent angle between nth C–D bond vector and the bilayer normal (Zhao et al. 2011). Clearly, in spite of a distinct physical significance of the order parameter and shape parameter, it is interesting to note that both parameters are derived from conformational details of individual membrane lipids. Therefore, it may be possible to compare the shape parameter of a lipid molecule with its order parameter at a specified nth carbon position, where n is the position of carbon showing a maximum angle (or value closer to 90°) between the C–D bond vector and the bilayer normal. As an example, let us consider a saturated (cylindrical) lipid that usually has a shape parameter ~ 1.0. Since cylindrical lipids are more ordered, one can expect an order parameter close to 1.0 since the parallel angle (or angle near 0°) between the C–D vector and the bilayer normal will be close to 0. On the other hand, an unsaturated lipid with a small hydrophilic head group (inverted truncated cone shape) usually has shape parameter >1.0, a value that increases with increasing unsaturation in acyl chains while keeping the head group size the same. As unsaturation of acyl chains leads to "disorder" in the bilayer, we expect a large dip in the value of the order parameter at the unsaturated carbon positions, as reported in the literature (Pandit et al. 2004; Zhao et al. 2008; Klauda et al. 2010). The order parameter value in this case would be close to 0 or −0.5. Thus, application of the geometrical approach developed by us in this work toward detailed analyses of order parameters of individual lipids may provide useful insights into the dynamics of the phase behavior of membranes. A combination of dynamics of the shape and order parameters of individual lipids in membranes is likely to provide deeper insights into the kinetic windows available for the development of localized domains of varying sizes, especially in the presence of different levels of compositional homogeneity (or heterogeneity).

Acknowledgments We thank Suhas Vasaikar and Chanchal Acharya at the Indian Institute of Technology for helpful discussions. S. B. is grateful for research fellowship support from the Council of Scientific and Industrial research, government of India. We are also very grateful to our anonymous reviewers for their invaluable inputs in improving the quality of our manuscript.

References

Allen FH (2002) The Cambridge structural database: a quarter of a million crystal structures and rising. Acta Crystallogr B 58: 380–388

Apajalahti T, Niemel P, Govindan PN, Miettinen MS, Salonen E, Marrink S-J, Vattulainen I (2010) Concerted diffusion of lipids in raft-like membranes. Faraday Discuss 144:411–430

Asp L, Kartberg F, Fernandez-Rodriguez J, Smedh M, Elsner M, Laporte F, Barcena M, Jansen KA, Valentijn JA, Koster AJ, Bergeron JJM, Nilsson T (2009) Early stages of Golgi vesicle and tubule formation require diacylglycerol. Mol Biol Cell 20:780–790

Bangham AD (1972) Model membranes. Chem Phys Lipids 8:386–392

Baumgart T, Hess ST, Webb WW (2003) Imaging coexisting fluid domains in biomembrane models coupling curvature and line tension. Nature 425:821–824

Cavalier-Smith T (2000) Membrane heredity and early chloroplast evolution. Trends Plant Sci 5:174–182

Chernomordik LV, Kozlov MM (2003) Protein–lipid interplay in fusion and fission of biological membranes. Annu Rev Biochem 72:175–207

Chernomordik LV, Kozlov MM, Melikyan GB, Abidor IG, Markin VS, Chizmadzhev YA (1985) The shape of lipid molecules and monolayer membrane fusion. Biochim Biophys Acta 812: 643–655

Chernomordik L, Leikina E, Cho M-S, Zimmerberg J (1995) Control of baculovirus gp64-induced syncytium formation by membrane lipid composition. J Virol 69:3049–3058

Christian DA, Tian A, Ellenbroek WG, Levental I, Rajagopal K, Janmey PA, Liu AJ, Baumgart T, Discher DE (2009) Spotted vesicles, striped micelles and Janus assemblies induced by ligand binding. Nat Mater 8:843–849

Christiansson A, Kuypers FA, Roelofsen B, Op Den Kamp JAF, Van Deenen LLM (1985) Lipid molecular shape affects erythrocyte morphology: a study involving replacement of native phosphatidylcholine with different species followed by treatment of cells with sphingomyelinase C or phospholipase A_2. J Cell Biol 101:1455–1462

Cicuta P, Keller SL, Veatch SL (2007) Diffusion of liquid domains in lipid bilayer membranes. J Phys Chem B 111:3328–3331

Collins MD, Keller SL (2008) Tuning lipid mixtures to induce or suppress domain formation across leaflets of unsupported asymmetric bilayers. Proc Natl Acad Sci USA 105:124–128

Cooke IR, Deserno M (2006) Coupling between lipid shape and membrane curvature. Biophys J 91:487–495

Davis CH, Nie H, Dokholyan NV (2007) Insights into thermophilic archaebacterial membrane stability from simplified models of lipid membranes. Phys Rev E 75:051921-1-6

Dickey A, Faller R (2008a) Examining the contributions of lipid shape and headgroup charge on bilayer behavior. Biophys J 95:2636–2646

Dickey A, Faller R (2008b) Behavioral differences between phosphatidic acid and phosphatidylcholine in the presence of the nicotinic acetylcholine receptor. Biophys J 95:5637–5647

Emoto K, Umeda M (2000) An essential role for a membrane lipid in cytokinesis: regulation of contractile ring disassembly by redistribution of phosphatidylethanolamine. J Cell Biol 149: 1215–1224

Feller SE, Venable RM, Pastor RW (1997) Computer simulation of a DPPC phospholipid bilayer: structural changes as a function of molecular surface area. Langmuir 13:6555–6561

Gurtovenko AA, Patra M, Karttunen M, Vattulainen I (2004) Cationic DMPC/DMTAP lipid bilayers: molecular dynamics study. Biophys J 86:3461–3472

Helfrich W (1973) Elastic properties of lipid bilayers: theory and possible experiments. Z Naturforsch C 28:693–703

Israelachvili JN, Mitchell DJ, Ninham BW (1976) Theory of self-assembly of hydrocarbon amphiphiles into micelles and bilayers. J Chem Soc Faraday Trans 72:1525–1568

Jimenez-Monreal AM, Villalain J, Aranda FJ, Gomez-Fernandez JC (1998) The phase behavior of aqueous dispersions of unsaturated mixtures of diacylglycerols and phospholipids. Biochim Biophys Acta 1373:209–219

Jo S, Lim JB, Klauda JB, Im W (2009) CHARMM-GUI membrane builder for mixed bilayers and its application to yeast membranes. Biophys J 97:50–58

Johannes L, Mayor S (2010) Induced domain formation in endocytic invagination, lipid sorting, and scission. Cell 142:507–510

Judson BL, Brown WJ (2009) Assembly of an intact Golgi complex requires phospholipase A_2 (PLA2) activity, membrane tubules, and dynein-mediated microtubule transport. Biochem Biophys Res Commun 389:473–477

Klauda JB, Venable RM, Freites JA, O'Connor JW, Tobias DJ, Mondragon-Ramirez C, Vorobyov I, MacKerell AD, Pastor RW (2010) Update of the CHARMM all-atom additive force field for lipids: validation on six lipid types. J Phys Chem B 114: 7830–7843

Kox AJ, Michels JPJ, Wiegel FW (1980) Simulation of a lipid monolayer using molecular dynamics. Nature 287:317–319

Kumar VV (1991) Complementary molecular shapes and additivity of the packing parameter of lipids. Proc Natl Acad Sci USA 88: 444–448

Kupiainen M, Falck E, Ollila S, Niemela P, Gurtovenko AA, Hyvonen MT, Patra M, Karttunen M, Vattulainen I (2005) Free volume properties of sphingomyelin, DMPC, DPPC, and PLPC bilayers. J Comp Theor Nanosci 2:401–413

Kusumi A, Koyama-Honda I, Suzuki K (2004) Molecular dynamics and interactions for creation of stimulation-induced stabilized rafts from small unstable steady-state rafts. Traffic 5:213–230

Lazaridis T, Mallik B, Chen Y (2005) Implicit solvent simulations of DPC micelle formation. J Phys Chem B 109:15098–15106

Lee GM, Ishihara A, Jacobson KA (1991) Direct observation of Brownian motion of lipids in a membrane. Proc Natl Acad Sci USA 88:6274–6278

Lipowsky R (1992) Budding of membranes induced by intramembrane domains. J Phys II (France) 2:1825–1840

Marrink S-J, Berger O, Tieleman P, Jahnig F (1998) Adhesion forces of lipids in a phospholipid membrane studied by molecular dynamics simulations. Biophys J 74:931–943

Marsh D (1996) Intrinsic curvature in normal and inverted lipid structures and in membranes. Biophys J 70:2248–2255

Martin W, Muller M (1998) The hydrogen hypothesis for the first eukaryote. Nature 392:37–41

Meer GV, de Kroon AIPM (2011) Lipid map of the mammalian cell. J Cell Sci 124:5–8

Mittal A, Grover R (2010) Self-assembly of biological membranes into 200–400 nm aqueous compartments. J Nanosci Nanotechnol 10:3085–3090

Mittal A, Leikina E, Bentz J, Chernomordik LV (2002) Kinetics of influenza hemagglutinin mediated membrane fusion as a function of technique. Anal Biochem 303:145–152

Mukherjee S, Soe TT, Maxfield FR (1999) Endocytic sorting of lipid analogues differing solely in the chemistry of their hydrophobic tails. J Cell Biol 144:1271–1284

Osman C, Voelker DR, Langer T (2011) Making heads or tails of phospholipids in mitochondria. J Cell Biol 192:7–16

Pandit SA, Jakobsson E, Scott HL (2004) Simulation of the early stages of nano-domain formation in mixed bilayers of sphingomyelin, cholesterol, and dioleylphosphatidylcholine. Biophys J 87:3312–3322

Patra M, Karttunen M, Hyvonen MT, Falck E, Lindqvist P, Vattulainenz I (2003) Molecular dynamics simulations of lipid bilayers: major artifacts due to truncating electrostatic interactions. Biophys J 84:3636–3645

Patra M, Karttunen M, Hyvonen MT, Falck E, Vattulainenz I (2004) Lipid bilayers driven to a wrong lane in molecular dynamics simulations by subtle changes in long-range electrostatic interactions. J Phys Chem B 108:4485–4494

Pecheur EI, Martin I, Maier O, Bakowsky U, Ruysschaert JM, Hoekstra D (2002) Phospholipid species act as modulators in p97/p47-mediated fusion of Golgi membranes. Biochemistry 41:9813–9823

Rasmussen S, Bedau MA, Chen L, Deamer D, Krakauer DC, Packard NH, Stadler PF (2009) Protocells: bridging nonliving and living matter. MIT Press, Cambridge

Roux A, Cuvelier D, Nassoy P, Prost J, Bassereau P, Goud B (2005) Role of curvature and phase transition in lipid sorting and fission of membrane tubules. EMBO J 24:1537–1545

Schafer LV, Marrink SJ (2010) Partitioning of lipids at domain boundaries in model membranes. Biophys J 99:L91–L93

Seelig A, Seeling J (1974) The dynamic structure of fatty acyl chains in a phospholipid bilayer measured by deuterium magnetic resonance. Biochemistry 13(23):4839–4845

Sharma P, Varma R, Sarasij RC, Gousset K, Krishnamoorthy G, Rao M, Mayor S (2004) Nanoscale organization of multiple GPI-anchored proteins in living cell membranes. Cell 116:577–589

Shillcock JC, Lipowsky R (2005) Tension-induced fusion of bilayer membranes and vesicles. Nat Mater 4:225–228

Suits F, Pitman MC, Feller SE (2005) Molecular dynamics investigation of the structural properties of phosphatidylethanolamine lipid bilayers. J Chem Phys 122:244714-1-9

Szule JA, Fuller NL, Rand RP (2002) The effects of acyl chain length and saturation of diacylglycerols and phosphatidylcholines on membrane monolayer curvature. Biophys J 83:977–984

Tanford C (1973) The hydrophobic effect: formation of micelles and biological membranes. Wiley-Interscience, New York

Tanford C (1978) The hydrophobic effect and the organization of living matter. Science 200:1012–1018

Tieleman DP, Berendsen HJC (1998) A molecular dynamics study of the pores formed by *Escherichia coli* OmpF porin in a fully hydrated palmitoyloleoylphosphatidylcholine bilayer. Biophys J 74:2786–2801

Tieleman DP, Sansom MSP, Berendsen HJC (1999) Alamethicin helices in a bilayer and in solution: molecular dynamics simulations. Biophys J 76:40–49

Tieleman DP, van der Spoel D, Berendsen HJC (2000) Molecular dynamics simulations of dodecylphosphocholine micelles at three different aggregate sizes: micellar structure and chain relaxation. J Phys Chem B 104:6380–6388

Veatch SL, Keller SL (2003) Separation of liquid phases in giant vesicles of ternary mixtures of phospholipids and cholesterol. Biophys J 85:3074–3083

Zaitseva E, Yang ST, Melikov K, Pourmal S, Chernomordik LV (2010) Dengue virus ensures its fusion in late endosomes using compartment-specific lipids. PLoS Pathog 6:e1001131

Zhao W, Rog T, Gurtovenko AA, Vattulainen I, Karttunen M (2007) Atomic-scale structure and electrostatics of anionic

palmitoyloleoylphosphatidylglycerol lipid bilayers with Na^+ counterions. Biophys J 92:1114–1124

Zhao W, Rog T, Gurtovenko AA, Vattulainen I, Karttunen M (2008) Role of phosphatidylglycerols in the stability of bacterial membranes. Biochimie 90:930–938

Zhao LN, Chiu S-W, Benoit J, Chew LY, Mu Y (2011) Amyloid β peptides aggregation in a mixed membrane bilayer: a molecular dynamics study. J Phys Chem B 115:12247–12256

Zimmerberg J, Kozlov MM (2006) How proteins produce cellular membrane curvature. Nat Rev Mol Cell Biol 7:9–19